



ELSEVIER

Journal of Nuclear Materials 290–293 (2001) 1097–1101

**journal of
nuclear
materials**

www.elsevier.nl/locate/jnucmat

Tolerable ELMs at high density in DIII-D

A.W. Leonard^{a,*}, T.H. Osborne^a, M.E. Fenstermacher^b, C.J. Lasnier^b,
M.A. Mahdavi^a

^a General Atomics, P.O. Box 85608, San Diego, California 92186-5608 USA

^b Lawrence Livermore National Laboratory, Livermore, CA 94551 USA

Abstract

The energy released at each edge-localized mode (ELM) is found to decrease in relation to the pedestal pressure, by more than a factor of five, as the line-averaged density in DIII-D H-mode is raised from about half the Greenwald density limit to near the Greenwald limit. The pedestal pressure remains nearly constant over this range demonstrating an attractive regime for future larger tokamaks. The reduction in ELM energy, in both low and high triangularity configurations, is seen to scale more with the pedestal electron temperature than the pedestal density. At low density both the electron density and temperature inside the separatrix drop due to the ELM instability; however at high density the density perturbation remains similar while the temperature profile is unaffected. ELMs at high density are also characterized by smaller magnetic fluctuations consistent with a higher toroidal mode number ELM instability. © 2001 Elsevier Science B.V. All rights reserved.

Keywords: DIII-D; ELM; Power deposition; Plasma edge

1. Introduction

Edge-localized modes (ELMs) remain a serious concern for future large tokamaks. The ELM instability relieves the plasma pressure gradient that builds just inside the separatrix and releases energy and particles into the scrape-off-layer (SOL) in a very short time, <1 ms [1,2]. The very large transient heat flux due to individual ELMs can lead to divertor surface ablation and unacceptable target plate erosion [3]. A previous multi-machine study [4] of low to moderate density H-mode found that the energy released at each ELM was approximately 1/3 of the pedestal electron energy. The pedestal energy is defined as the pedestal pressure times the plasma volume. The conclusion of this result was somewhat discouraging in that high pedestal values desired for good confinement in future large tokamaks could lead to unacceptable divertor target erosion.

A few regimes of small and attractive ELMs have subsequently been identified [5]. Type III ELMs [6] typically are very small in amplitude and often occur when the heating power is only slightly above that necessary to maintain H-mode. However, in this regime the edge pedestal is often lower and confinement is degraded. A particularly attractive regime is that of Type II [7,8], or grassy, ELMs. For this regime, the edge pedestal and global confinement remain high, but ELMs are very small and irregular. Type II ELMs appear to occur at high triangularity, high elongation, and perhaps high density. Because these ELMs are not well understood they are currently being carefully studied and evaluated.

In this paper, we extend the previous work of Type I ELMs to examine ELM behavior at higher density. While the previous study examined Type I ELMs at about half of the Greenwald density, future tokamaks are expected to operate at close to the Greenwald density to maximize fusion power output, and it is important to determine ELM behavior in this higher density regime. The Greenwald density, n_{GW} , is a commonly observed density limit in tokamaks and is defined as $n_{GW} \text{ (m}^{-3}\text{)} = 10^{14} I_p / \pi a^2$, where I_p (amps) is the plasma current and a (m) is the plasma minor radius. Previous

* Corresponding author. Tel.: +1-619 455 2214; fax: +1-619 455 4156.

E-mail address: leonard@fusion.gat.com (A.W. Leonard).

work has shown that Type I ELM energy may become smaller at higher density [4,9]. Here we study this relationship in detail and find that as density increases the energy lost at each ELM becomes smaller in relation to the pedestal pressure. These ELMs are small enough that future tokamaks could operate with a large pedestal and still not threaten the divertor target due to ELM heat flux. A description of the experimental setup is described in the next section. The scaling of ELM energy and other characteristics with increasing density is presented in Section 3. Finally a discussion of the results and remaining work for scaling to larger tokamaks is given in Section 4.

2. Experimental set-up and diagnostics

For these experiments, deuterium gas puffing is used to vary the plasma density in H-mode while keeping other parameters fixed, primarily the plasma current of 1.2 MA and toroidal field of 2.0 T. These lower-single-null (LSN) discharges are in a low triangularity private flux pumping configuration which is found to produce steady conditions more easily and allow higher density operation without reverting to L-mode. Two cases are studied, a low triangularity case of $\delta \sim 0.0$, Fig. 1(a), and a higher triangularity case of $\delta \sim 0.36$, Fig. 1(b). The higher triangularity and its associated higher stability limit is used to separate variations of pedestal density and temperature.

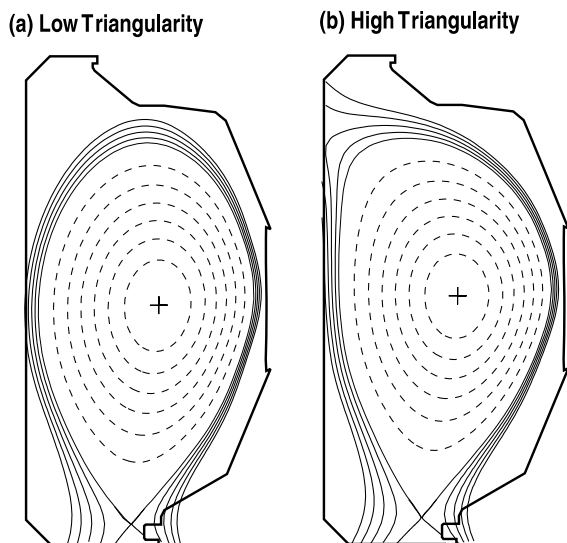


Fig. 1. The magnetic configurations used for these experiments. The divertor geometry is optimized for pumping of the private flux region. The lower half triangularity is constant at $\delta \sim 0.1$, while the upper triangularity is changed between (a) at $\delta = 0.0$ and (b) $\delta = 0.36$.

Density scans are performed by varying the gas puff rate from discharge to discharge. Nearly steady-state edge conditions result allowing for an extended period to make pedestal and ELM measurements. The plasma stored energy is calculated every 0.5 ms in a time window selected for fast magnetic data acquisition. The ELM energy is determined by evaluating the difference in the plasma stored energy 1.5 ms before and after each ELM, with a fast rise in the divertor H_α signal indicating the time of each ELM. The noise and uncertainty in this measurement is typically about 5 kJ for each ELM.

The edge electron temperature, density and pressure profiles both before and after an ELM for both low and high density, as shown in Fig. 2, are measured with a Thomson scattering system collecting a profile every

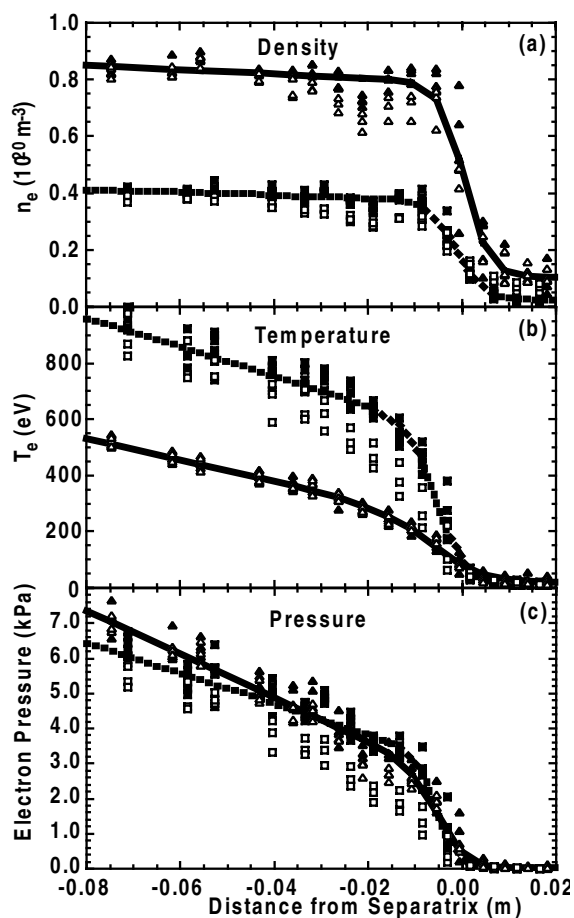


Fig. 2. Edge profiles collected within 1.5 ms before (closed symbols) and 1.5 ms after (open symbols) an ELM from Thomson scattering. The profiles are fitted with a tanh function to determine the pedestal values. Shown are the (a) density, (b) electron temperature, (c) the electron pressure. The triangle symbols and solid tanh fitting line are for high density. The dashed line and square symbols represent low density.

12 ms. The pre-ELM profiles are gathered by collecting all the Thomson data, within a steady-state data window, that falls within 1.5 ms before the onset of the ELM instability. The Thomson data is then mapped to the mid-plane. The pedestal values, $n_{e,ped}$, $T_{e,ped}$, and $P_{e,ped}$, are then determined by fitting the collected profiles to a tanh function in the edge and a linear profile inside the steep gradient region. The post-ELM profiles are collected in a similar data window, but after each ELM.

3. Experimental results

The relationship of ELM energy to pedestal pressure is the important aspect under study in this paper. Future tokamaks will require both a large edge pedestal pressure for confinement and small ELMs to protect the divertor. A previous study [10] of the pedestal and confinement in this configuration showed the pedestal pressure remained relatively constant up to a density of $n_{e,ped} \sim 70\text{--}75\%$ of n_{GW} . This corresponds to a line-averaged density of about 95% of n_{GW} for both low and high triangularity discharges. The high triangularity configuration with its increased ideal edge stability achieves nearly a factor of two higher pedestal pressure for densities below the degradation threshold. In terms of the pedestal temperature, $T_{e,ped}$, the pedestal begins to degrade at $T_{e,ped} \sim 300$ eV for low triangularity and $T_{e,ped} \sim 500$ eV at high triangularity.

As density is raised the ELM energy becomes smaller in relation to the pressure pedestal. This reduction is summarized in Fig. 3(a) where the ELM energy ratio decreases with increasing pedestal density. In Fig. 3, ΔW_n is defined as the energy lost at each ELM divided by the pedestal electron energy, or $P_{e,ped}$, times the plasma volume. As $n_{e,ped}$ increases ΔW_n decreases continuously until the ELM size is within the measurement uncertainty. Also shown in Fig. 3 is the value of ΔW_n previously obtained from the multi-machine scaling at a density of $\sim 40\%$ of n_{GW} . As the pedestal pressure is constant up to $n_{e,ped} \sim 70\%$ n_{GW} any reduction in the ΔW_n below $n_{e,ped} \sim 70\%$ n_{GW} represents an absolute reduction in ELM size. The parameters at the pedestal degradation threshold then represent an attractive regime for future tokamaks with a robust pedestal, tolerable ELMs and line-averaged density approaching n_{GW} .

The value of ΔW_n at a given $n_{e,ped}$ can vary considerably from the low to the high triangularity configuration. Density is apparently not the sole determining factor for ELM size. In Fig. 3(b), the ELM data is plotted versus the pedestal electron temperature, $T_{e,ped}$. Here the data from the low and high triangularity cases lie along the same curve. This data indicates that $T_{e,ped}$, or some process more closely associated with temperature, is critical in controlling the amplitude of the ELM instability.

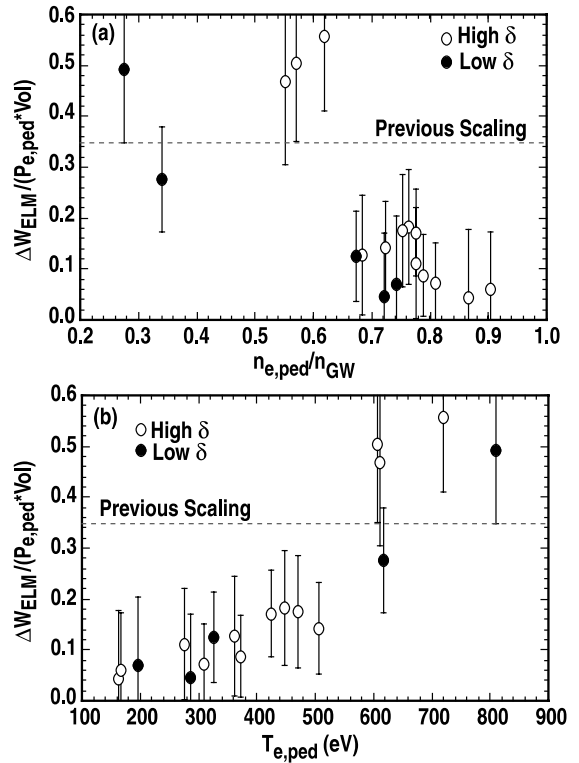


Fig. 3. ΔW_n , the ELM energy normalized by the pedestal electron energy, plotted as a function of (a) the pedestal density, and (b) the pedestal electron temperature.

In order to gain insight into the mechanisms controlling the ELM size it is useful to examine details of the ELM itself. In Fig. 2, the edge electron density, temperature, and pressure profiles are plotted just before and after an ELM for the low triangularity case. The closed symbols are collected from the Thomson scattering system less than 1.5 ms before an individual ELM, with the open symbols representing profiles less than 1.5 ms after an ELM. The solid lines are tanh fits through the pre-ELM profiles at high density while the dashed lines are fits through low density profiles. At low density the ELM perturbs the profile far inside the separatrix. The density drops quickly by 20–30% to about 4 cm inside the separatrix at the mid-plane. At high density the pedestal density drops at the ELM a similar amount, but the perturbation does not extend as far inside the separatrix, only 2–3 cm. The differences between high and low density ELMs show up particularly in perturbations to the T_e profile, as shown in Fig. 2(b). The T_e profile at low density is significantly perturbed by the ELM inside the separatrix. However at high density almost no change can be observed in the T_e profile after an ELM. These profiles are combined in Fig. 2(c) to plot the ELM perturbation to the pressure

profile, which should be directly related to the ELM energy loss. At low density the ELM causes a drop in $P_{e,ped}$ by up to 50%. This perturbation extends inside the pedestal up to about 5 cm inside the separatrix. At high density, however, the ELM perturbation to the pressure is much more modest and extends inside the separatrix only slightly past the pedestal. Summarizing, it appears that at low density the ELM transports significant energy and particles from inside the separatrix, and pedestal, into the SOL. However, at high density only density is carried across the separatrix due the ELM, and the perturbation is limited to near the pedestal region.

The magnetic fluctuations obtained from Mirnov probes also display distinct differences between low and high density ELMs. At low density the magnetic fluctuations increase at the start of the rise in H_x , and quickly grow reaching a peak at the same time as the peak in the H_x signal. The ELM instability then quickly ends resulting in a rapid drop in the magnetic fluctuation level and a slower drop in the H_x level. For the high density case, the magnetic fluctuations during the ELM are smaller, by a factor of 8–10, than for low density. In fact, the fluctuations rise only slightly above the background noise level. The duration of the fluctuations is ~ 300 μ s in all cases.

The reduction in magnetic fluctuation level can rise from two effects. First the ELM instability may saturate at a lower level at high density. This would result in a lower ELM energy at higher density if the ELM instability duration does not change. Another possibility is a change in the mode structure itself. Because the magnetic probes are located away from the magnetic surface of the ELM instability the magnetic fluctuations will fall off as r^{-m} , where m is the mode number of the ELM instability. If at high density the mode number of the instability increases, then the radial extent of the perturbation will be smaller leading to lesser transport. This reduced ELM energy may occur even though the fluctuation level at the resonant surface is the same as the low density case. In our case, both the instability amplitude and mode number may be playing a role in reducing the ELM energy loss at high density.

4. Discussion

In order to scale the ELM energy loss to future large tokamaks a model is needed that incorporates the physical mechanism controlling the ELM amplitude. It is unlikely that n_e or T_e alone is controlling the ELM instability, but parameters such as collisionality, resistivity and neutral flux may be important. Also the large variability in individual ELMs makes it difficult to determine the ELM scaling from the present results without a physical model as a guide. Following is a discussion of several physical mechanisms that could

possibly affect the ELM instability. Further work will be required to determine the importance of these effects.

A common model for increased transport during an ELM is that magnetic instabilities grow until modes overlap producing a stochastic magnetic topology in the high gradient region. Parallel transport would then allow a high flux of energy across the separatrix into the SOL. Since parallel heat conduction is such a strong function of electron temperature, $T_3^{7/2}$, rapid energy transport would cause a quick drop in electron temperature significantly inside the separatrix. This may be the type of transport that is responsible for the drop in T_e as seen in the low density case. Another possibility for transport is that growing instabilities eventually lead to magnetic reconnection carrying plasma across the separatrix. This convective transport would likely not perturb the electron temperature as much as conductive transport. The high density ELMs may be a transition from conductive to convective transport. In order to study and understand the ELM transport a better model of the instability itself is needed.

One model of edge stability in H-mode [11] utilizes the large edge bootstrap current due to the steep pressure gradient of the H-mode barrier. The bootstrap current reduces the magnetic shear in the pedestal and stabilizes the higher order pressure driven ballooning modes. The pressure gradient may then rise until lower mode number current/pressure driven modes become unstable. The lower order modes may be more virulent and produce a bigger perturbation because they can grow to larger amplitude before saturation and island overlap. Also the mode penetrates further inside the plasma because the magnetic perturbation does not drop off as rapidly as the higher order modes. As density increases the resulting higher collisionality reduces the edge bootstrap current. This might lead to destabilization of higher order pressure driven modes at a lower pressure gradient than the lower order modes. The level of reduced pressure gradient at higher order mode onset must still be determined by further modeling.

There are other effects which might also be playing a role in the scaling of ELM amplitude. Increasing resistivity with a lower electron temperature could slow the growth rate of the modes. Another factor could be neutral fueling in the pedestal region. These and other effects need to be investigated before a definitive scaling can be determined.

5. Summary

We have shown that as density increases in DIII-D the ELMs of H-mode become much more rapid and of smaller amplitude. The energy transported across the separatrix by individual ELMs at high density are more than five times smaller than the previous multi-machine

scaling at lower density. If the ELMs of future large tokamaks are also five times smaller than the low density scaling then future divertor targets should tolerate the associated heat pulses, while maintaining a robust pedestal. However, it is not yet possible to accurately scale these optimistic results to larger tokamaks until the underlying mechanisms are identified. This might be accomplished by comparison of experimental results with modeling and theory and further multi-machine experimental comparisons.

Acknowledgements

Work supported by US Department of Energy under Contracts DE-AC03-99ER54463 and W-7405-ENG-48.

References

- [1] P. Gohil, M.A. Mahdavi, L.L. Lao, et al. Phys. Rev. Lett. 61 (1989) 1603.
- [2] H. Zohm, T.H. Osborne, K.H. Burrell et al., Nucl. Fus. 35 (1995) 543.
- [3] H.D. Pacher, E9. Disruption and ELM Erosion, Appendix E9, Section 1.7 (Divertor), ITER Design Description Document, ITER No. G 17 DDD 1 96-08-21 W2.1, August 1996.
- [4] A.W. Leonard, A. Herrmann, K. Itami et al., J. Nucl. Mater. 266–269 (1999) 109.
- [5] H. Zohm, Plasma Phys. Control. Fus. 38 (1996) 105.
- [6] W. Suttrop, Plasma Phys. Control. Fus. 42 (Suppl. 5A) (1999) A1.
- [7] Y. Kamada, T. Oikawa, L. Lao et al., Plasma Phys. Control. Fus. 42 (Suppl. 5A) (1999) A247.
- [8] T. Ozeki, M.S. Chu, L.L. Lao et al., Nucl. Fus. 30 (1990) 1425.
- [9] W. Suttrop, O. Gruber, B. Kurzan et al., Plasma Phys. Control. Fus. 42 (Suppl. 5A) (1999) A97.
- [10] T.H. Osborne, J.R. Ferron, M.E. Fenstermacher et al., Plasma Phys. Control. Fus. 42 (Suppl. 5A) (1999) A175.
- [11] J.R. Ferron, M.S. Chu, G.L. Jackson et al., Phys. Plasmas 7 (2000) 1976.